Materials Science in Semiconductor Processing 27 (2014) 404–411

Contents lists available at ScienceDirect

Materials Science in Semiconductor Processing

journal homepage: www.elsevier.com/locate/mssp

Band gap engineering by substitution of S by Se in nanostructured $CdS_{1-x}Se_x$ thin films grown by soft chemical route for photosensor application

Farha Y. Siddiqui [a], Shaheed U. Shaikh [a], Deepali J. Desale [a], Deepak S. Upadhye [b], Sandeep V. Mahajan [b], Anil V. Ghule [b], Pankaj Varshney [a], Sung-Hwan Han [c], Ramphal Sharma [a,b,*]

[a] Thin film and Nanotechnology Laboratory, Department of Physics, Dr. Babasaheb Ambedkar Marathwada University, Aurangabad 431004, M. S., India
[b] Department of Nanotechnology, Dr. Babasaheb Ambedkar Marathwada University, Aurangabad-431004, M. S., India
[c] Nano material Lab, Department of chemistry, Hanyang University Seoul, 133-791, South Korea

ARTICLE INFO

Keywords:
Thin film
X-ray diffraction
Optical properties
Electrical properties
Soft chemical route

ABSTRACT

Ternary alloys of $CdS_{1-x}Se_x$ ($x=0$, $x=0.2$, $x=0.4$, $x=0.6$, $x=0.8$, $x=1$) thin films were prepared on to glass substrates by a simple and economical soft chemical route (chemical bath deposition) at 50° to 80 °C in air. The as-grown films were characterized by optical and electrical measurement systems, X-ray diffraction (XRD), Energy dispersive X-ray analysis (EDAX) and SEM (scanning electron microscopy). The optical study reveals shift in the absorption edge towards the higher wavelengths, i.e. the band gap decreases as a function of '*x*' (quantity of selenium in the bath). *I–V* measurement of CdS (resulted when $x=0$), $CdS_{1-x}Se_x$ ($x=0.2$, $x=0.4$, $x=0.6$, $x=0.8$) and CdSe (resulted when $x=1$) thin films under dark and illumination conditions (60 W) were measured. Increase in photoconductivity is observed, suggesting its applicability in photosensor devices. Electrical resistivity shows semiconducting behavior and activation energy decreases. The XRD patterns reveals that deposited thin films have hexagonal mixed structure. EDAX confirmed the compositional parameters. SEM images showed uniform deposition of the material over the entire glass substrate.

1. Introduction

Semiconductor compounds from II–VI group are very important materials in view of their photosensitivity, photoconductivity and thermoelectric power for photosensor applications [1]. Most of the photosensors consist of semiconductors having good electrical conductance which varies depending upon the intensity of radiation striking the material. Typical photoconductive materials consist of germanium, gallium, selenium, compounds like cadmium sulfide, bismuth sulfide, oxides, selenides and composites [2,3]. CdS and CdSe are two very popular semiconductors belonging to II–VI group. CdSSe is used in wide range of applications in optoelectronics devices such as optically bistable elements, optical switches, transistors, modulators, laser diodes, optical harmonic generators, and optical memories [4]. It is also used

* Corresponding author at: Thin film and Nanotechnology Laboratory, Department of Physics, Dr. Babasaheb Ambedkar Marathwada University, Aurangabad-431004, (M. S.), India.
Tel.: +91 9422793173; +91 240 2401365;
fax: +91 240 2403115, +91 240 240333.
E-mail address: ramphalsharma@yahoo.com (R. Sharma).

http://dx.doi.org/10.1016/j.mssp.2014.07.014
1369-8001/

because of their potential application in conversion of solar energy into electrical energy [5] and in variety of semiconductor devices. The choice of photoconducting material is usually between CdS in which very high sensitivity is possible but response time is high and CdSe in which a lower response time is possible at the cost of some loss in sensitivity [6]. If we consider CdS and CdSe separately energy band gaps are 2.4 eV [7] and 1.7 eV [8], respectively. The tunability of these semiconductors can be achieved through the composition modulation [9,10]. For example, ternary alloy of semiconductor $CdS_{1-x}Se_x$ and some other alloys with continuously tuned band gap have been reported consequently [11]. Wavelength tunable emission can be attained from ternary compounds by simple adjustment of composition [12,13]. Thus with this motivation to develop a photosensor material with the ideal band gap to achieve high mobility and long life time of the charge carriers, in the present work, we contend the possibility of producing new semiconducting material using CdS and

Table 1
Tabulation form of band gaps of $CdS_{1-x}Se_x$ thin film in eV.

Composition	Band gap (eV)
CdS	2.42
$CdS_{0.8}Se_{0.2}$	2.16
$CdS_{0.6}Se_{0.4}$	2.03
$CdS_{0.4}Se_{0.6}$	1.97
$CdS_{0.2}Se_{0.8}$	1.8
CdSe	1.73

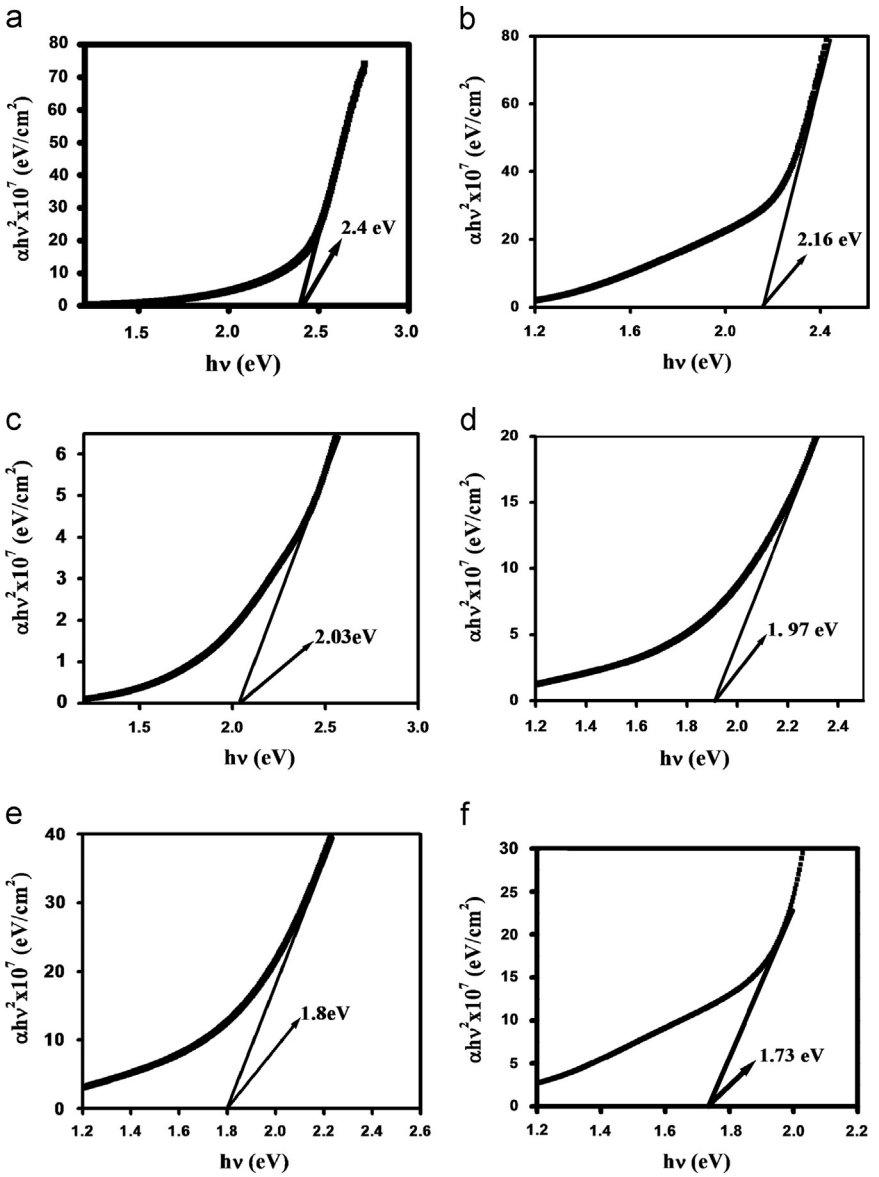

Fig. 1. Representative Plot of $(\alpha h\nu)^2$ verses $h\nu$ to estimate energy band gap of as deposited (a) CdS, (b) $CdS_{0.8}Se_{0.2}$, (c) $CdS_{0.6}Se_{0.4}$, (d) $CdS_{0.4}Se_{0.6}$, (e) $CdS_{0.2}Se_{0.8}$ and (f) CdSe thin films, respectively.

CdSe. $CdS_{1-x}Se_x$ alloy thin film can be grown by the techniques such as the chemical bath deposition method [14,15], an electrodedeposition method [16], the physical vapor transport method [17], nucleation and crystal growth mechanism [18] etc.

In view of this, present paper the ternary $CdS_{1-x}Se_x$ alloy thin film with variable composition of 'x' is considered, where 'x' is the composition of selenium. $x=0$, $x=0.2$, $x=0.4$, $x=0.6$, $x=0.8$ and $x=1$ thin films are prepared using simple soft chemical route (chemical bath deposition method). Various preparative parameters, such as ionic concentration, temperature and pH were optimized to get good quality thin films on glass substrates.

Table 2
Tabulation form of photosensitivity in $CdS_{1-x}Se_x$ thin film in percentage.

Composition	Photosensitivity (%)
CdS	18
$CdS_{0.8}Se_{0.2}$	54
$CdS_{0.6}Se_{0.4}$	27
$CdS_{0.4}Se_{0.6}$	35
$CdS_{0.2}Se_{0.8}$	47
CdSe	87

2. Experimental details

$x=0$, $x=0.2$, $x=0.4$, $x=0.6$, $x=0.8$, and $x=1$ thin films were grown by chemical bath deposition. We optimized

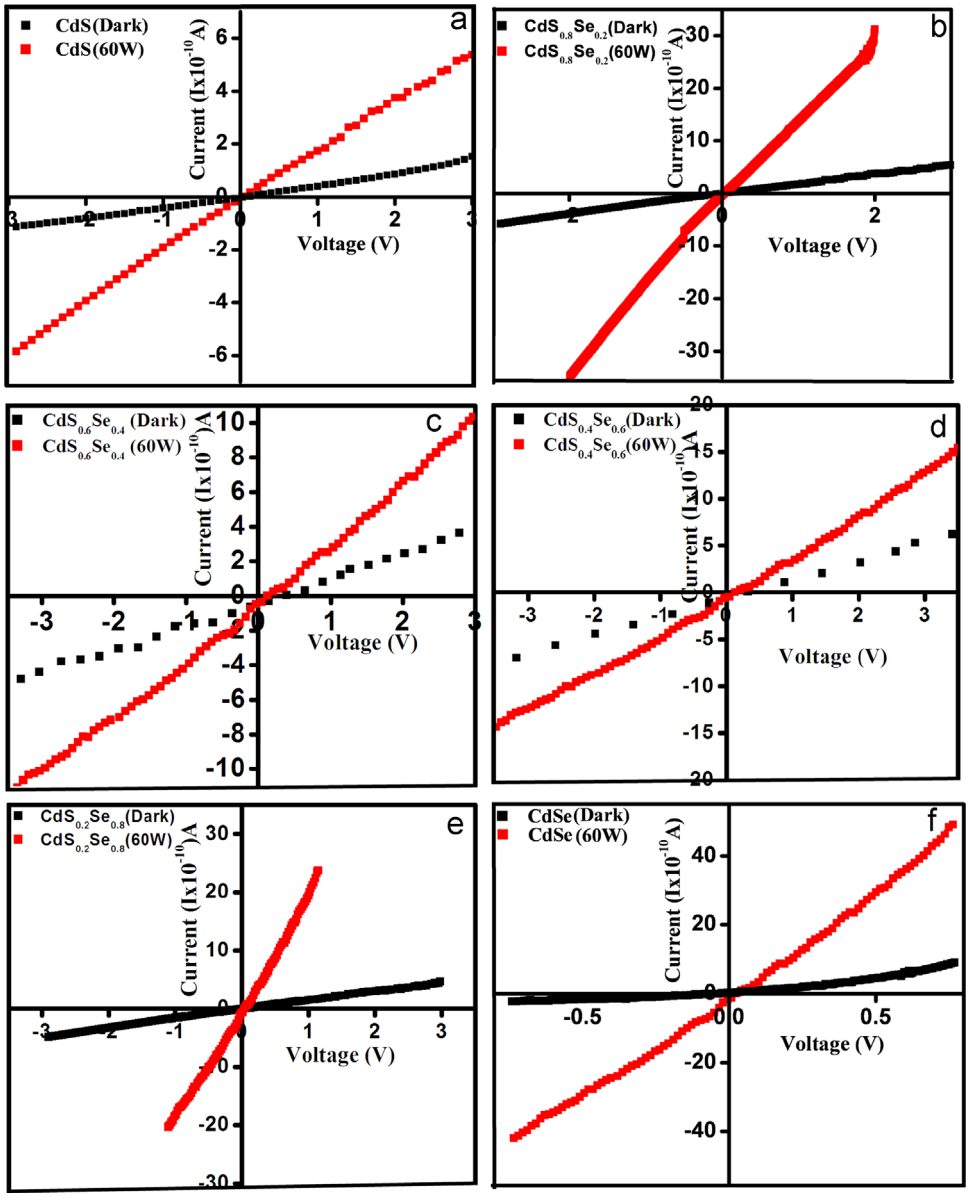

Fig. 2. Representative *I–V* plots obtained from as deposited (a) CdS, (b) $CdS_{0.8}Se_{0.2,}$ (c) $CdS_{0.6}Se_{0.4}$, (d) $CdS_{0.4}Se_{0.6}$, (e) $CdS_{0.2}Se_{0.8}$ and (f) CdSe thin films, respectively under dark and illumination condition (60 W).

the preparative parameters such as reaction temperature, deposition time, pH, and molarity using $CdSO_4$, thiourea, and selenium solution on glass substrates. The temperature of the $CdS_{1-x}Se_x$ solutions was kept at 50 °C for the period of 1 h. The pH of the solution was maintained at ~11.5 to obtain $CdS_{1-x}Se_x$ thin films and all were prepared considering different volumes of reactants that are thiourea and selenium solution.

2.1. Deposition of CdS thin film

CdS thin resulted when $x=0$. For this equal volume of the solutions i.e. $CdSO_4$ and thiourea (20 mL) were taken considering the molarity of $CdSO_4$ solution as 0.1 M and for thiourea 0.2 M. The pH of the resultant mixture was kept at ~11.5 by addition of ammonia. The temperature of the reaction bath was maintained at 80 ± 5 °C and the deposition was carried out for the period of 1 h.

2.2. Deposition of CdSe thin film

CdSe thin resulted when $x=1$. In this case the procedure is similar as that of the deposition of the CdS thin film, but the difference is that instead of thiourea, selenium (sodium selenosulphate) solution was used. 20 mL solution $CdSO_4$ was treated with 20 mL of selenium solution (sodium selenosulphate). The pH of the resultant mixture was ~11.5 using ammonia. The bath temperature was maintained at 50 ± 5 °C for the period of 1 h.

2.3. Deposition of $Cds_{1-x}Se_x$ thin film

For this the volume of $CdSO_4$ was kept same as before (20 mL) and the volume of thiourea and selenium (sodium selenosulphate) was varied, giving $x=0.2$, 0.4, 0.6, and 0.8. The pH of the resultant mixture was ~11.5 by adding ammonia. The bath temperature was maintained at 50 ± 5 °C for the period of 1 h.

3. Characterization techniques

Optical absorption studies were carried out using UV–vis (Perkin-Elmer, Lambda-25) spectrophotometer in the range 400–1100 nm. Photosensitivity of the samples was studied using *I–V* system interfaced with computer. Resistivity measurements were done using the two probe method. Structural analysis was done using X-ray diffraction (XRD) with a Bruker (AXS-D8 ADVANCE) X-ray diffractometer in the range $2\theta=20$–60° having CuKα_1 ($\lambda=1.5405$ Å).Energy dispersive X-ray analysis (EDAX). Surface morphology of the ternary alloy $CdS_{1-x}Se_x$ thin films were carried out using scanning electron microscopy (SEM).

4. Result and discussion

4.1. Optical studies

In the present investigation, optical absorption by $CdS_{1-x}Se_x$ thin films were studied in the wavelength range of 400–1100 nm. It is observed that the optical absorption edge is shifted towards the longer wavelength with increase in composition of 'x'. The nature of the transition (direct or indirect) is determined by using the relation.

$$\alpha=\alpha_0(h\nu-E_g)^n/h\nu \quad (1)$$

where E_g the energy difference between valence and conduction band and n is a constant equal to 1/2 for direct band gap materials and 2 for indirect band gap material. The natures of the plots indicate the existence of direct transitions. The bandgap E_g is determined by extrapolation of the straight portion of the plot to the energy axis as shown in Fig. 1.

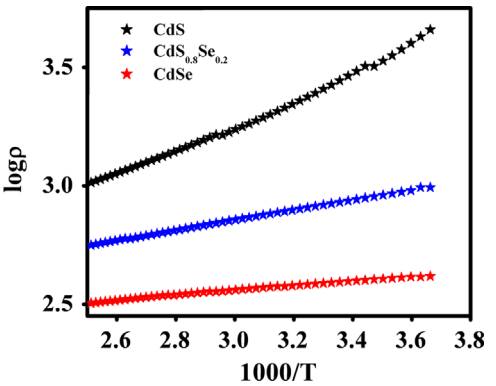

Fig. 4. Plot showing logρ verses 1000/T of as deposited CdS, $CdS_{0.8}Se_{0.2}$ and CdSe thin films.

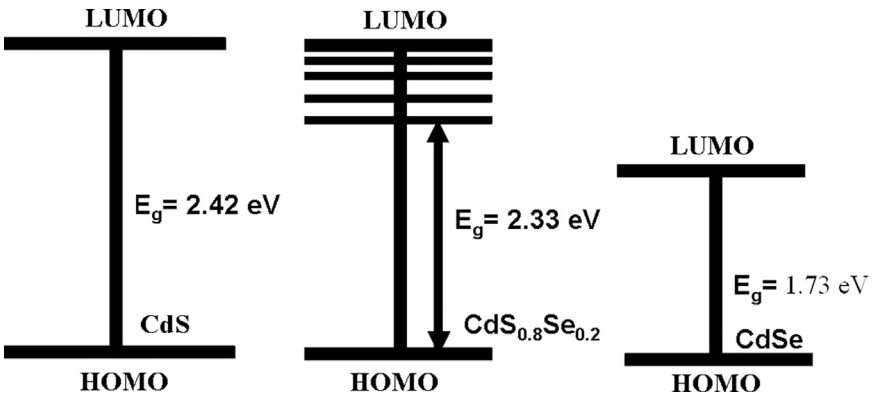

Fig. 3. Schematic representation of the formation of localized states in CdS on addition of 'Se'.

The band gaps of the $CdS_{1-x}Se_x$ as a function of x are shown in Table 1 [19,20], in which it is observed that the band gap of $CdS_{0.8}Se_{0.2}$, $CdS_{0.6}Se_{0.4}$, $CdS_{0.4}Se_{0.6}$, and $CdS_{0.2}Se_{0.8}$ thin film is in between the individual band gaps of CdS and CdSe [21]. So this decrease in band gap may be due to the presence of localized states in the forbidden gap. The width of mobility edge depends on the degree of disorder and defects present in the structure. In solids unsaturated bonds are responsible for the formation of these defects. Such defects produce localized states in the forbidden gap. The presence of such states is responsible for the decrease of optical band gap [22]. Therefore the films prepared with different ratios of 'S' and 'Se' show a monotonic variation in the band gap with the composition, indicating the formation of a common lattice of CdSSe thin film.

4.2. Photosensor characteristics

Fig. 2 shows the *I–V* characteristics of the as deposited $CdS_{1-x}Se_x$ thin films, respectively, in dark and illumination conditions (60 W/cm^2). The *I–V* curves are straight lines passing through the origin indicating ohmic behavior. The effect of light on the samples can be seen in said figure. It is seen that current is proportional to the applied voltage which means it satisfies the Ohm's law confirming the ohmic nature. On illumination photocurrent is observed to increase, this may be related to increase in carrier concentration. The excitation of the electrons from valance band to the conduction band significantly improves the electrical conductivity of the semiconductor. When the film is exposed to light, number of charge carriers increases by several orders of magnitude. The photo generated current increases due to increase in conductivity. These results indicate enhancement of conductivity of the material and therefore the phenomenon is known as photoconductivity or photosensing.

The photosensitivity of the samples were calculated using the formula

$$S = Rd - Rl/Rd \quad (2)$$

Where

R_d = resistance of thin film in dark
R_l = resistance of thin film in the presence of light

It is found that the photosensitivity increases from CdS to CdSe, which is due to excitation of charge carrier when the photons were incident on the sample. The photosensitivity was calculated as mentioned in Table 2. We found that the photosensitivity in $CdS_{0.8}Se_{0.2}$, is more than other compositions which may be due to the reason that CdS

Table 3
Tabulation form of presence of Cd, S and Se in CdS, $CdS_{0.8}Se_{0.2}$, and CdSe thin films in percentage.

Composition	Atomic percentage in the film by SEM–EDAX analysis (%)		
	Cd	S	Se
CdS	82	18	0
$CdS_{0.8}Se_{0.2}$	70	22	8
CdSe	63	0	37

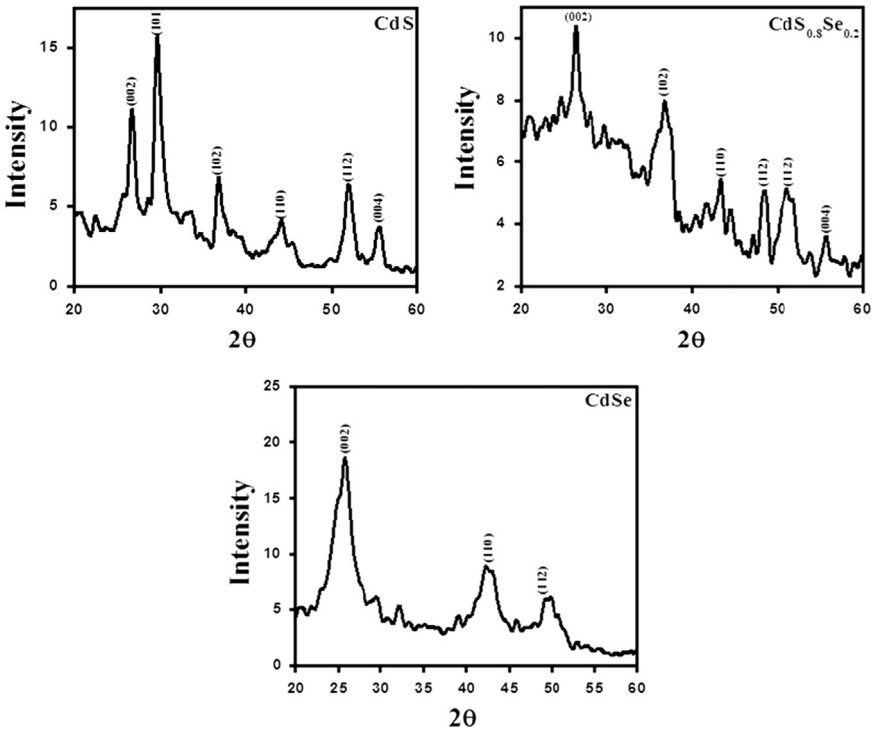

Fig. 5. Representative XRD pattern of as deposited CdS, $CdS_{0.8}Se_{0.2}$ and CdSe thin films.

have very high sensitivity but response time is also high and in CdSe lower response time is possible at the cost of some loss in sensitivity. As per the result of photosensitivity characteristics the most suitable composition is $CdS_{0.8}Se_{0.2}$, therefore we further investigated CdS, $CdS_{0.8}Se_{0.2}$ and CdSe for other properties. The schematic representation of CdS, $CdS_{0.8}Se_{0.2}$, and CdSe nano structured thin films along with their energy band gap as Homo - Lumo and the formation

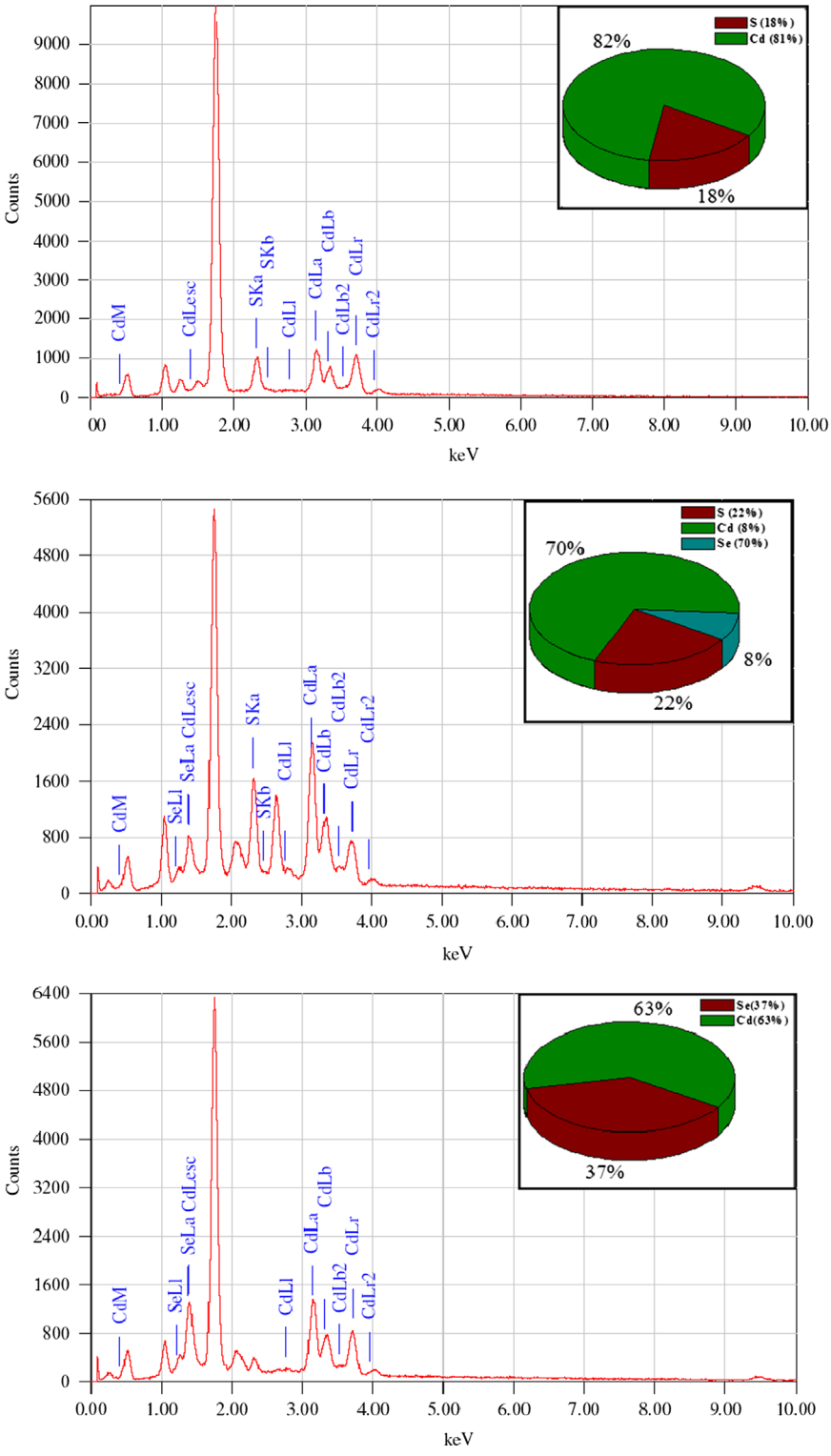

Fig. 6. Representative EDAX spectra of as deposited CdS, $CdS_{0.8}Se_{0.2}$ and CdSe thin films.

of localized states in CdS on addition of 'Se' is shown in Fig. 3.

4.3. Electrical properties

The electrical resistivity of CdS, CdSe, and $CdS_{0.8}Se_{0.2}$ thin films was studied using dc the two-point probe method. The variation of log (ρ) versus 1000/T is shown in Fig. 4. It is observed that the resistivity decreases with increase in temperature, which indicates the semiconducting nature of the thin film [23]. Furthermore, the activation energy of the films was obtained using equation

$$\rho = \rho_0 \exp(E_a/KT) \quad (3)$$

where ρ is resistivity at temperature at T, ρ_0 is a constant, k is Boltzmann constant and E_a is the activation energy, which is estimated by the slope of the log (ρ) versus $1/T$. The resistivity values were found to be 0.97×10^3 Ωcm for CdS, 0.053×10^3 Ωcm for $CdS_{0.8}Se_{0.2}$ and 0.0×10^3 Ωcm for CdSe thin films, respectively i.e. resistivity of CdS is more than CdSe thin film [24]. The calculated values of activation energies are 0.1788 eV, 0.1019 eV and 0.0622 eV for CdS, $CdS_{0.8}Se_{0.2}$ and CdSe, respectively.

4.4. Structural and compositional study

Fig. 5 shows the GI-XRD pattern of CdS, $CdS_{0.8}Se_{0.2}$ and CdSe. CdS shows the orientation along (002), (101), (102), (110), (112) and (400) planes which were assigned in accordance with the standard JCPDS data reference card of CdS (file no: 80-0006) confirms its nanocrystalline nature with hexagonal phase[24–26].

CdSe shows the orientations along (002), (110) and (112) planes and confirms the hexagonal structure [27] assigned with JCPDS data reference card of CdSe (file no: 77-2307). The XRD spectrum of $CdS_{0.8}Se_{0.2}$ shows maximum peaks of CdS and minimum peaks of CdSe this indicates the presence of selenium in the film, which is also confirmed by the EDAX. Extra peaks are nothing but humps of the glass substrate used for deposition of the thin film. The crystallite size was calculated using Scherer's formula,

$$D = k\alpha/\beta \cos\theta \quad (4)$$

where the constant K is a shape factor usually 0.94, λ the wave length of X-ray (0.15418 nm), β the FWHM in radians and θ is the Bragg's angle. The crystallite size of CdS, $CdS_{0.8}Se_{0.2}$ and CdSe were found to be 139 nm, 111 nm and 46 nm, respectively.

The chemical composition of $CdS_{0.8}Se_{0.2}$ was confirmed by EDAX. The elemental analysis was carried out only for Cd, S and Se and the average atomic percentage ratio of Cd: S: Se is listed in Table 3. Fig. 6 shows the representative EDAX spectra only for three compositions i.e. CdS, $CdS_{0.8}Se_{0.2}$ and CdSe. It shows that the composition in the film is same as in the reaction bath mixture. However, there were some additional peaks in the EDAX spectra, this could be attributed to Si, O, Ca, Mg, etc., arising due to the presence of these elements in the amorphous glass used as substrate.

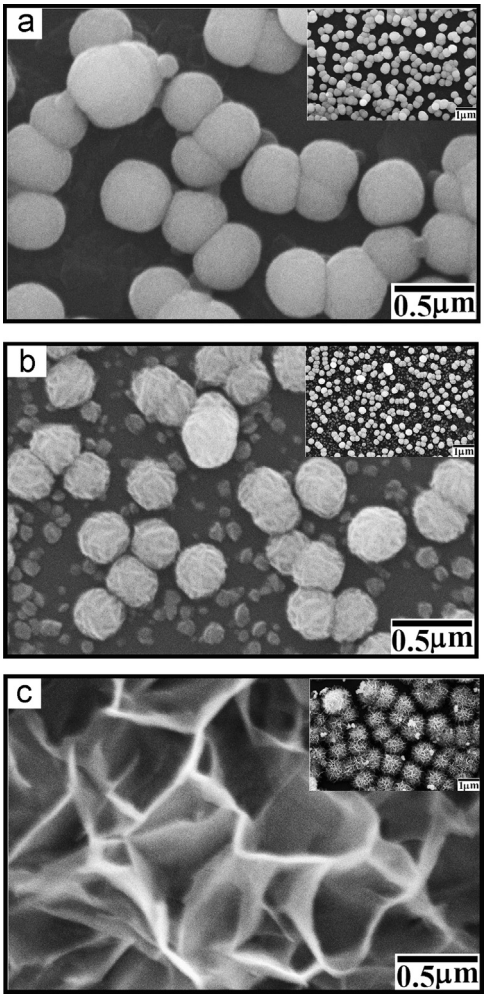

Fig. 7. Representative SEM images of as deposited CdS, $CdS_{0.8}Se_{0.2}$ and CdSe thin films.

4.5. Surface morphological analysis

Fig. 7 shows the SEM micrographs of CdS, $CdS_{0.8}Se_{0.2}$ and CdSe. The SEM micrographs of all the films show uniform surface morphology over the entire glass substrate surface. Nearly, all the grains were spherical in shape. It is also seen from the SEM images that all the samples consists of a dense layer with small crystallites The SEM image 7(a) shows the surface morphology of CdS thin film. Image 7(c) clearly depicts that CdSe thin film surface morphology show uniformly deposited flower like nanostructure. Whereas Fig. 7(b) shows the surface morphology of $CdS_{0.8}Se_{0.2}$ in which both spherical shaped and flower like nanocrystalline structure can be seen.

5. Conclusion

$CdS_{1-x}Se_x$ thin films have been successfully deposited by chemical bath deposition technique. The optical property reveals the red-shift of the absorption edge which reveals that the edge shifts towards the longer wavelength, as we consider from CdS to CdSe, which convey that the

band gap decreases form CdS (resulted when $x=0$) to CdSe (resulted when $x=1$). Furthermore, all the samples showed good response to the light. The electrical study confirms that the resistivity decreases with the addition of selenium in the CdS thin film. XRD study of $CdS_{0.8}Se_{0.2}$ thin film confirms the formation hexagonal phase with nanocrystalline nature, Presence of selenium is supported by EDAX study. SEM shows the formation of spherical shaped CdS and flower like CdSe nanocrystalline Structure, whereas $CdS_{0.8}Se_{0.2}$ shows both spherical shaped and flower like nanocrystalline structure. From the studies stated above the ternary alloy $CdS_{1-x}Se_x$ thin films due to their wide and fine tunability of the band gap have potential applications in various opto-electronic devices.

Acknowledgment

F.Y. Siddiqui acknowledges, UGC, New Delhi for providing fellowship and financial support in the form of research IUAC project Ref. No: EST/DEPT/2011/5191-95. We are thankful to the Director, IUAC, New Delhi, CSR Indore, Hanyang University Seoul, South Korea and Dept. of Physics Dr. B. A. M. University Aurangabad for providing lab facilities.

References

[1] C.S. Ferekides, U. Balasubramanian, R. Mamazza, V. Viswanathan, H. Zhao, D.L. Morel, Sol. Energy 77 (2004) 823–830.
[2] R.R. Ahire, A.A. Sagade, N.G. Deshpande, S.D. Chavhan, R. Sharma, F. Singh, J. Phys. D: Appl. Phys. 40 (2007) 4850–4854.
[3] V.N. Semnov, O.S. Ostapenko, A.N. Lukiin, E.I. Zavrazhnov, Inorg. Mater. 36 (2000) 1197–1199.
[4] V. Abhishek, N. Swati, K.P. Praveen, P.K. Bhatnagar, P.C. Mathur, J. Nanopart. Res. 9 (2007) 1125–1131.
[5] V.M. Bhuse, Mater. Chem. Phys. 106 (2007) 250–255.
[6] P.K.C. Pillai, N. Shroff, A.K. Tripathi, J. Phys. D: Appl. Phys. 16 (1983) 393–399.
[7] M. Karimi, M. Rabiee, F. Moztarzadeh, M. Tahriri, M. Bodaghi, Curr. Appl. Phys. 9 (2009) 1263–1268.
[8] L.K. Yu, H.J. Jae, H.K. Kyung, S.Y. Hyun, S.S. Man, H.B. Se, K. Yong, Nanotechnology 20 (2009) 095605–0956011.
[9] A. Pan, Y. Hua, Y. Richeng, Z. Bingsuo, Nanotechnology 17 (2006) 1083–1086.
[10] A. Pan, Y. Lide, Q. Yong, Y. Yang, S.K. Dong, Y. Richeng, Z. Bingsuo, W. Peter, Z. Margit, G. Ulrich, Nano Lett. 8 (2008) 3413–3417.
[11] K. Harishchandra Sadekar, A.V. Ghule, R. Sharma, J. Alloys Compd. 509 (2011) 5525–5531.
[12] A. Pan, H. Yang, R. Liu, R. Yu, B. Zou, Z. Wang, J. Am. Chem. Soc. 127 (2005) 15692–15693.
[13] T. Zhai, X. Zhang, W. Yang, Y. Ma, J. Wang, Z. Gu, D. Yu, H. Yang, J. Yao, Chem. Phys. Lett. 427 (2006) 371–374.
[14] R.S. Mane, C.D. Lokhande, Mater. Chem. Phys. 65 (2000) 1–31.
[15] J.B. Chaudhari, N.G. Deshpande, Y.G. Gudage, A. Ghosh, V.B. Huse, R. Sharma, Appl. Surf. Sci. 254 (2008) 6810–6816.
[16] Y. Liang, L. Zhai, X. Zhao, D. Xu, J. Phys. Chem. B 109 (2005) 7120–71203.
[17] U.N. Roy, Y. Cui, C. Barnett, K.T. Chen, A. Burger, T.G. Jonathan, J. Electron. Mater. 31 (2002) 791–794.
[18] R.S. Sonawane, S.D. Naik, S.K. Apte, M.V. Kulkarni, B.B. Kale, Bull. Mater. Sci. 31 (2008) 495–499.
[19] J.C. Young, S.H. In, H.P. Jae, N. Sahn, G.P. Jae, Nanotechnology 17 (2006) 3775–3778.
[20] S.J. Castillo, A. Mendoza-Galvan, R. Ramırez-Bon, F.J. Espinoza-Beltran, M. Sotelo-Lerma, J. Gonzalez-Hernandez, G. Martınez, Thin Solid Films 373 (2000) 10–14.
[21] R.C. Kainthla, D.K. Pandya, K.L. Chopra, J. Electrochem. Soc. 129 (1982) 99–102.
[22] G. Lakshminarayana, M. Piasecki, G.E. Davydyuk, G.L. Myronchuk, O.V. Yakymchuk, O.V. Parasyuk, I.V. Kityk, Mater. Chem. Phys. 135 (2012) 837–841.
[23] A. Ubale, S. Shirbhate, J. Alloys Compd. 497 (2010) 228–233.
[24] R.S. Mane, C.D. Lokhande, Thin Solid Films 304 (1997) 56–60.
[25] M.A. Mahdi, S.J. Kasem, J.J. Hassen, A.A. Swadi, S.K.J. Al-ani, Int. J. Nanoelectron. Mater. 2 (2009) 163–172.
[26] I. Kaur, D.K. Pandya, K.L. Chopra, J. Electrochem. Soc. 127 (1980) 943–948.
[27] P.P. Hankare, S.D. Delekar, M.R. Asabe, P.A. Chate, V.M. Bhuse, A.S. Khomane, K.M. Garadkar, B.D. Sarwade, J. Phys. Chem. Solids 67 (2006) 2506–2511.